Lumped elements circuit of terahertz fishnet-like arrays with composite dispersion

Jorge Carbonell, Charles Croënne, Frédéric Garet, Eric Lheurette, Jean-Louis Coutaz, Didier Lippens

Lumped elements circuit of terahertz fishnet-like arrays with composite dispersion

Cite as: J. Appl. Phys. **108**, 014907 (2010); https://doi.org/10.1063/1.3455994
Submitted: 08 April 2010 • Accepted: 20 May 2010 • Published Online: 13 July 2010

Jorge Carbonell, Charles Croënne, Frédéric Garet, et al.

Lumped elements circuit of terahertz fishnet-like arrays with composite dispersion

Jorge Carbonell,[1,a)] Charles Croënne,[2] Frédéric Garet,[3] Eric Lheurette,[2] Jean Louis Coutaz,[3] and Didier Lippens[2]
[1]*Departamento de Ingeniería Electrónica, Wave Phenomena Group, Universidad Politécnica de Valencia, Camino de Vera, s/n, 46022 Valencia, Spain*
[2]*Institut d'Électronique de Microélectronique et Nanotechnologies, Université des Sciences et Technologies de Lille, Avenue Poincaré BP 60069, 59652, Villeneuve d'Ascq Cedex, France*
[3]*Laboratoire IMEP-LAHC, UMR 5130 du CNRS, Université de Savoie, 73376, Le Bourget du Lac Cedex, France*

(Received 8 April 2010; accepted 20 May 2010; published online 13 July 2010)

We have analyzed and characterized a terahertz stacked holes array over a broad transmission bandwidth. In this context, we identify the key contributions of the surface plasmon modes related to the periodicity of array, and of the subcut off transmission through the holes responsible of a ground left-handed dispersion branch. The experimental verification of a multimode electromagnetic behavior is performed by time domain spectroscopy, with a complementary assessment by full-wave analysis. A circuitlike approach appears suitable for the understanding of a zero-gap transition between the left- and right-handed characteristics, opening the way of nonvanishing group velocity in a near-zero index propagation medium. Such a balanced composite operation, pointed out over the past in the dual element transmission line approaches, is thus generalized for a stacked subwavelength holes array, whose operation can be compared to the one of the so-called fishnet structures. © *2010 American Institute of Physics*. [doi:10.1063/1.3455994]

I. INTRODUCTION

Front side illuminated devices operating at terahertz and even higher frequencies have become a very active field of research owing to their wide range of possible applications. In particular, devices exhibiting a negative refractive index may open the path to obtain high-resolution lenses, super scatters, and other challenging purposes. Several routes have been explored to fulfill a normal incidence requirement such as the ones based on the so-called nanorod[1] or fishnet[2,3] approaches. In addition, the works of other groups were based on stacked subwavelength holes arrays perforated in metallic plates with air-filled spacer layers.[4,5] With this type of configuration, some of the authors just demonstrated the left-handedness of a subwavelength holes arrayed stack with an operating frequency around 0.5 THz.[6] The experiments were performed by coherent time domain spectroscopy (TDS), and they evidenced a ground left-handed dispersion branch via the frequency variations in phase and magnitude of the transmission coefficient. The good agreement between full-wave calculations of the transmission and experimental data was subsequently used in order to retrieve the dispersion characteristics. These studies have pointed out the importance of the stacking, with at least two elemental layers, and of the shape of the holes with an optimized elliptical aspect ratio of 1.7:1. They also show the possibility to move ahead toward a balanced composite behavior, namely a seamless transition (no gap) between the ground left-handed dispersion branch and the right-handed one. Over the past, such a property was first pointed out in composite transmission lines with a dual configuration with respect to conventional lines by loading them with series capacitances and shunt inductances.[7,8] By including the equivalent lumped elements of the interconnecting sections it was also shown that a balanced composite behavior can be achieved provided that the resonance frequencies of the shunt and series equivalent circuits are equal. In the present work, we address the problem of a composite behavior in the aforementioned stack of subwavelength holes arrays, which can be illuminated under front side conditions, and not with a grazing incidence as in our previous works.[9] To this aim and as mentioned previously for transmission lines, we will establish an equivalent circuit description. In a way similar to transverse electromagnetic mode propagation description in a two-conductor transmission line, we will see that the electromagnetic properties are here the result of contributions of both surface and evanescent modes. Recently, a lumped element approach was successfully applied to single frequency selective surfaces (FSSs),[10–12] by using parallel LC resonant circuits. This equivalent circuit description is actually able to describe extraordinary transmission through subwavelength holes arrays. In the present work, we show that coupling phenomena via multiple modes, related to the array periodicity, is responsible for the left-(LH) and right-handed (RH) character of the various transmission bands, and this dual behavior can be directly derived from the equivalent circuit description. In the following, we briefly review the background on the design and fabrication of the prototype that we have characterized. We provide additional experimental data in connection with the measurement of the reflection coefficient not reported previously.[6] We then provide a comprehensive interpretation of the wide band transmission response derived

[a)]Electronic mail: jorcarol@upvnet.upv.es.

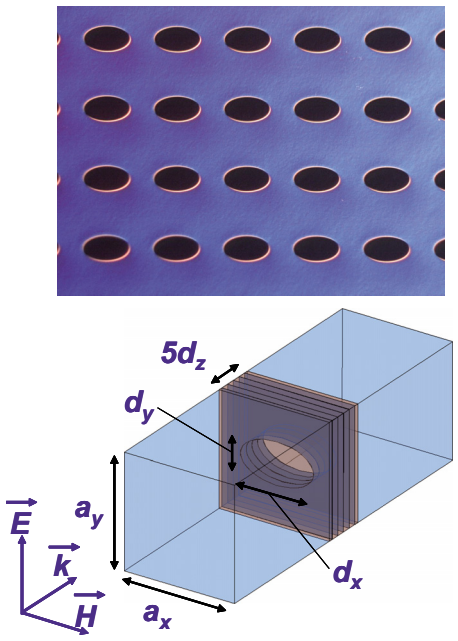

FIG. 1. (Color online) Optical microscope view of the surface of the fabricated prototype, units in μm (a), and unit cell schematic of the arrayed five layer stacked microstructure with design dimensions and the impinging wave polarization (b). Dimensions as follows: $a_x=a_y=340$ μm, $d_x=1.7d_y=238$ μm, $d_y=140$ μm, and $d_z=30$ μm (average value).

from the multiple modes which are involved. The modal analysis serves as a basis for a precise explanation of the transmission characteristics with an approach based on an equivalent circuit description, which is finally compared to the experimental characteristics.

II. PROTOTYPE DESIGN, FABRICATION, AND MEASUREMENT

Figure 1 shows an optical microscope picture (zoomed front view) of the fabricated device and a schematic of the basic cell in the propagation direction (periodic boundary conditions apply for the modeling). The dimensions were chosen with the goal of achieving a high transmission level around 500 GHz. They also take into account the monolithic fabrication capabilities and the limitations in the metal/dielectric structuring techniques. This is in contrast to the prototypes with thick metal layers of several millimeters which have been fabricated at millimeter waves. Thin films of gold (0.4 μm) are here microstructured with elliptical-shaped holes. This anisotropy of the unit element of the surface permits one to improve the transmitted level by enlarging the non critical axis of the hole, namely the one orientated along the magnetic field vector.[6] Benzocyclobutene (BCB, with $\varepsilon_r=2.6$) dielectric layers with an average thickness of 30 μm are used as spacers between the metallic plates. Further details on the fabrication process and on the transmission characteristic for a five layers prototype can be found in Ref. 6. Measured results were obtained by TDS in a pump probe configuration. We complete here the experimental data with the reflection measurement carried out on the same prototype and which was not given in that reference.

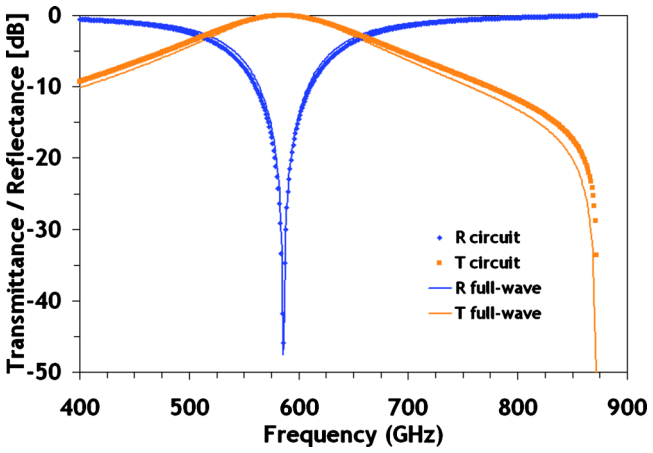

FIG. 2. (Color online) Transmittance and reflectance characteristics of a single metallic layer structure. Results show a comparison between full-wave simulations and equivalent circuit.

III. MODAL ANALYSIS OF THE BROAD BAND TRANSMISSION CHARACTERISTIC

Full-wave analysis shows the involvement of several surface modes related to the transverse periodicity of the array and to the characteristics of the BCB interlayers. Coupling of surface modes through the dielectric spacer takes place as long as the separation between metallic layers is small compared to the attenuation length of the surface waves of the metal–dielectric interfaces.[13] These modes appear in addition to the resonant mode whose characteristic frequency is directly related to the hole size. In order to analyze the propagation modes step by step, we consider in the following first a single layer and then a multilayered structure.

Figure 2 shows transmittance and reflectance, calculated by means of the finite element commercial code high frequency structure simulator (HFSS) by Ansoft of a single layer in the propagation direction (same dimensions as in Fig. 1). In this case, a gold metallic layer is sandwiched between two BCB slabs of thickness 15 μm. A relatively broad bandwidth transmission window with a high transmission level is centered on 590 GHz (gold is modeled with finite conductivity $\sigma=4.1\times10^7$ S/m). A zero of transmission can also be noted at 870 GHz which can be attributed to a Rayleigh anomaly,[14] related to a_y the transverse periodicity,[10] which becomes multiple of the wavelength. It will be shown that this frequency dependence of a single layer structure constitutes an envelope function for the multilayered stacked device. Even if this behavior has a resemblance with the one reported in Ref. 12 also for a single metallic screen, in that work the origin of the transmission maximum below the Rayleigh anomaly is attributed to an extraordinary transmission phenomenon. Basically, the transmission window displayed in Fig. 2 is related to the matching of half of the guided wavelength to the horizontal size (along x) of the elliptical hole. The guided wavelength is in this case smaller taking into account the dielectric constant of the BCB layer. At 590 GHz, $\lambda_g=\lambda_0/\sqrt{\varepsilon_r}=540$ μm. Therefore, this behavior is related to a classical FSS operation, and propagation through the surface is strongly related to the holes geometry.

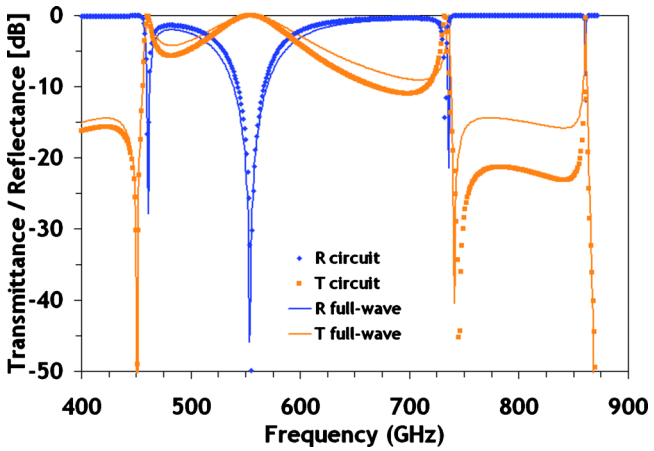

FIG. 3. (Color online) Transmittance and reflectance characteristics of a double layer stacked structure. Results show a comparison between full-wave simulations and equivalent circuit.

Moving now to the stacked layers case, it is of paramount importance to point out that the presence of the dielectric spacer layers between the metallic plates completely changes the device behavior as compared to an air-filled interlayer situation. In the single layer case, the effect of the dielectric slab surrounding the metallic layer will basically shift the transmission-reflection characteristics to lower frequencies. In the case of a multilayer device, and as already pointed out theoretically,[13] metal-dielectric interfaces will be involved in the rich dispersion relation describing propagation of surface waves. Part of the propagation characteristics have also been defined, using optical wording, as internal surface plasmons and external surface plasmons, employing the terminology of that work. They can, respectively, be defined as surface waves that propagate along the internal and external metal-dielectric interfaces of the stacked device, respectively.

A two layer simulation result (transmittance and reflectance) is plotted in Fig. 3. Geometrical parameters correspond again to those of Fig. 1. It can be observed that on top of the background characteristic describing the single layer case (Fig. 2), several resonant features appear at 460, 730, and 860 GHz.

Additionally, Fig. 4 helps to identify, through the E-field patterns, different modes involved in the transmittance characteristic. They can be associated to the microstructured metallic layers and to the coupling modes through the dielectric waveguide constituted by the BCB layer. At 468 GHz the TM_{02} mode generates a narrow LH transmission band. Backward wave propagation was identified via effective parameter retrieval from simulation results.[6] Generation of LH transmission bands through the TM_{02} mode, was also pointed out in the millimeter wave range.[4] At 554 GHz, the contribution of the FSS mode is clearly visible ($\lambda_g/2$ matching the transverse size of the hole), and generates a RH transmission band. At 734 GHz, the TM_{22} mode is generating a second RH branch. Let us note that these frequencies slightly decrease as the number of stacked layers increases. And this is also true when we compare the frequency of the main transmission window to the one of the single layer case. At 554 GHz, Fig. 4(b) the presence of the TM_{02} is also barely observable superimposed to the half-wavelength matched to the lateral size of the hole (x direction). A short comment will be provided in the following section to this phenomenon in terms of equivalent circuits.

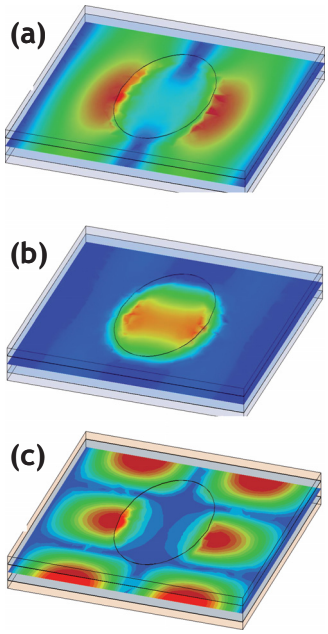

FIG. 4. (Color online) Maps of the E-field in the center of the spacer BCB layers corresponding to the ground LH branch [468 GHz–(a)], to the first RH branch [554 GHz–(b)], and to the second RH branch [734 GHz–(c)].

Internal couplings through the BCB dielectric spacers can therefore be attributed to distinct resonant contributions associated to the waveguide modes. Waveguide modes are related to the periodicity of the structure (a_x and a_y). Alternatively and through a complementary approach, they can be described as internal surface waves at the metal-dielectric interfaces.[13] Approximate expressions are given in that work to estimate the resonant frequencies of these "internal" modes (waveguide modes). Nevertheless, it is pointed out that the accuracy of the method is limited and also dependent on the perturbation introduced by the hole itself in the coupling parameters. In our case, that method would only provide a qualitative estimate of the resonant frequencies, since the large size of the elliptic holes strongly modifies the waveguide coupling frequencies. Therefore that method cannot provide in our case predicted values for the resonant coupling frequencies.

Other works have also analyzed these coupling modes in terms of electrical resonances involving LC circuits,[15,16] only at a conceptual level. This approach was explored in deeper details in Ref. 17, where an analytical model for propagation in stacked fishnet devices is presented. Although the physics governing this type of device is equivalent, that analytical model (which is also reinterpreted through an equivalent circuit) is developed in particular for small hole sizes, as compared to the transverse periodicity of the microstructure. Therefore, as it is underlined in Ref. 17, the model lacks of precision to describe the observed characteristics in our experimental results with large hole size.

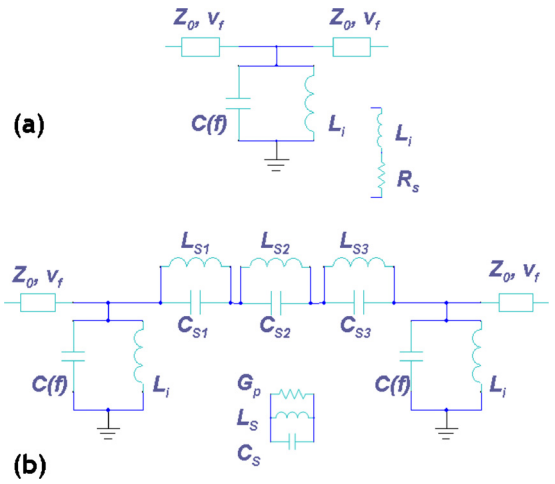

FIG. 5. (Color online) Schematic equivalent circuit modeling the unit cell of a perforated single metallic plate structure (a), and equivalent circuit modeling the coupling mechanism between two stacked perforated metallic plates (b). Insets show equivalent circuits to, respectively, account for metallic losses R_s in the inductive element L_i and for dielectric losses G_p in the spacers coupling circuit formed by L_s and C_s.

IV. EQUIVALENT CIRCUIT DESCRIPTION OF THE MULTIPLE LAYER STACKED HOLES ARRAY

For the circuit description of a single perforated metallic plate, we adopted the lumped element resonant circuit in Fig. 5(a), as initially proposed in Refs. 10 and 11. We successfully checked the accuracy of this description by comparing the frequency dependence of a single perforated screen (equivalent circuit and full-wave simulations) in previous Fig. 2. The inductance of the metallic screen L_i is roughly invariant with frequency, while the capacitance is given by the following equation:

$$C(f) = C_0 + \frac{K}{\sqrt{\omega_R^2 - \omega^2}}. \quad (1)$$

C_0 accounts for the higher order mode contributions to the hole capacitance, and K is a fitting parameter related to the amount of coupling mainly performed through the TM_{02} mode; ω_R is the Rayleigh's anomaly angular frequency.[10] Relationship with the TM_{02} mode was already pointed out in the description of Fig. 4(b). The resonant tank formed by L_i and $C(f)$ describes the generic FSS behavior of the single screen.

In a second stage, the coupling between two plates is modeled by means of resonant parallel circuits (L_sC_s) as depicted in Fig. 5(b). Each coupling resonant mode contribution is defined by a corresponding LC resonant tank. Therefore, a number of series connected tanks will be necessary to model each one of the high-order resonant modes. This model can hence handle multiple-mode coupling and provides quantitative information in terms of transmittance and reflectance (both in magnitude and phase). Metal and dielectric losses can be, respectively, accounted for by a resistance R_s in series with L_i and a leakage conductance G_p in parallel with C_s (insets of Fig. 5). Values for these loss elements can be empirically determined, by fitting the simulation or experimental results. Let us note, however that loss elements

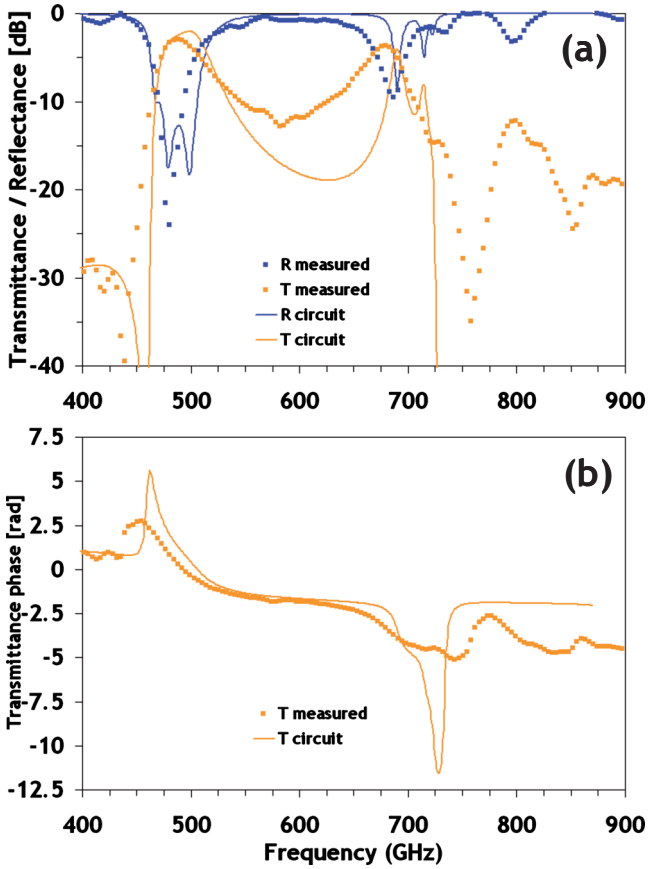

FIG. 6. (Color online) (a) Transmittance and reflectance for a five layer stacked structure in magnitude and (b) in unwrapped transmission phase. Equivalent circuit response is displayed with solid lines and measured results are displayed with symbols.

have realistic values according to the employed materials and geometry, and to the operation frequencies. Validity of this equivalent circuit is limited to the frequency range below Rayleigh's anomaly (around 880 GHz for the prototype dimensions). This basically covers the spectrum portion where there is single mode propagation in the air-filled waveguide forming the unit cell of the device. Let us nevertheless note that, in the regions filled by the BCB dielectric higher order modes may propagate, even if they are evanescent in the air-filled access regions of the simulation domain of Fig. 1.

Figure 6(a) compares the frequency dependence of the reflection and transmission coefficients measured by terahertz-TDS with the frequency response achieved by the circuit approach, for a five layer stack. The variation in the transmittance unwrapped phase is also compared in Fig. 6(b). A relatively good agreement is achieved supporting the suitability of such a circuit approach. Most of the discrepancies are a consequence of the tolerances of the technological process,[6] in particular discrepancies in the alignment and thickness of the vertically stacked layers and possible bend of the sandwiched structure due to the stress in the thick BCB layers. At this stage, all cells in the equivalent circuit are considered identical, but it is nevertheless confirmed that the prototype has different thicknesses for the stacked dielectric spacers. Despite these issues, we underline the good agreement found between both results.

After an optimization based on the curve fitting of the

TABLE I. Equivalent circuit values for the five layer microstructure.

C_0 (fF)	L_{s1} (nH)	L_{s2} (pH)	L_{s3} (pH)
3.71	4.41	1.18	0.46
K (mF)	C_{s1} (fF)	C_{s2} (fF)	C_{s3} (fF)
7.04	27.2	39.85	84.42

full-wave simulation results in successively stacked number of layers, the values found for the lumped elements in the equivalent circuit are summarized in Table I.

FSS operation is governed by the fact that, at the maximum transmission (590 GHz for the single layer case), the LC tank formed by L_i and $C(f)$ is resonating. At this frequency, both inductive and capacitive contributions have equal intensity and the shunt equivalent circuit behaves as an open circuit. Hence, full transmission is obtained. Below that maximum transmission frequency, the behavior of this circuit is dominated by the inductive component L_i, the metallic layer is fundamentally inductive at low frequencies. And above the resonance frequency, the dominant element is the variable capacitance $C(f)$. Near Rayleigh's anomaly, the shunt capacitance tends to infinity and therefore the structure behaves as a short-circuit providing total reflection.

Moreover, the equivalent circuit description helps to understand the LH or RH character of the resonant features of the wide band transmission characteristic. In a few words, the inductive or capacitive character of the resonant tank modeling the metallic plate will drive the LH or RH character of the resonant features associated to the different resonant modes, see Fig. 7. Below the holes resonant frequency, an isolated metallic plate will have basically a shunt inductive behavior, whereas above it, the metallic plate behavior will be dominated by the variable shunt capacitance [Fig. 7(a)]. In a similar way, for each resonant series tank L_sC_s associated to each coupling mode, an inductive behavior is expected below its resonant frequency given by $\omega_s = 1/\sqrt{L_sC_s}$, and a capacitive behavior is expected above it. From this duality, and for the stacked layers case, it will immediately be derived that a series capacitive element (from the first coupling mode) combined with the shunt inductive behavior of the metallic plate will produce a LH band, below the holes resonant frequency [Fig. 7(b)].

At the resonance frequency $f_{s1}=451$ GHz, transmission is necessarily forbidden, but slightly above it the combination of a series capacitance (of the coupling circuit) and a shunt inductance (of the metallic layer) will generate the LH band. Conversely, a series inductive element combined with the dominant shunt capacitive element above the resonant frequency of the holes will produce a RH propagation window, for the second and third coupling modes. Slightly below the resonance frequencies, $f_{s2}=745$ GHz and $f_{s3}=869$ GHz (where transmission is null), the combination of a series inductance (of the coupling circuit) and a shunt capacitance (of the metallic layer) produces a RH band. This explains the fact that in the simulation results, the resonant

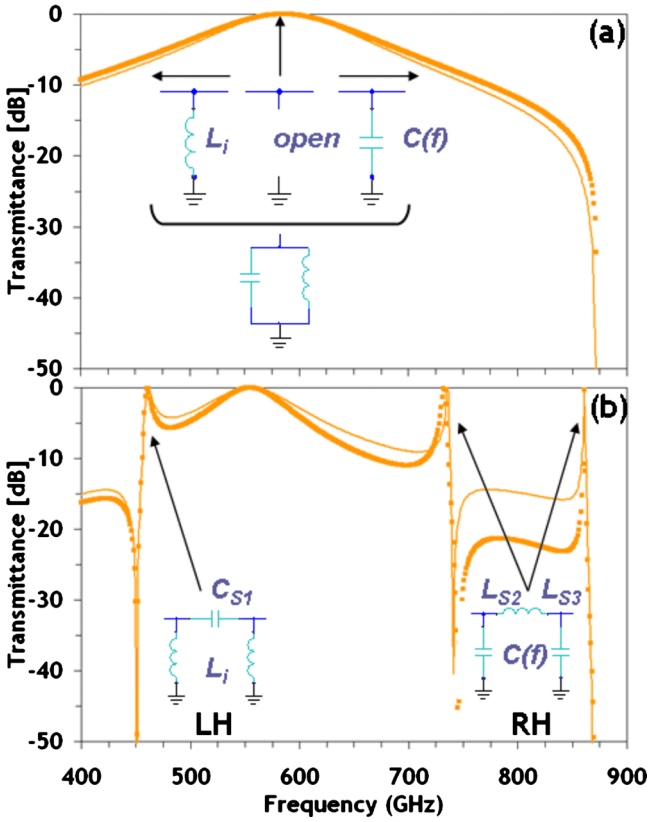

FIG. 7. (Color online) Transmittance for a single layer structure with in inset the dominant elements in the equivalent circuit description as a function of the frequency range. In (b), transmittance for a double layer structure (two metallic plates). The dominant elements of the equivalent circuits are displayed for each resonant feature associated to the coupling modes and the respective dominant element of the metallic plates. This qualitative description is defined either as left handed for the first coupling mode or right handed for the second and third coupling modes.

features associated to the waveguide modes have a transmission zero and a maximum transmission in different relative positions depending on whether transmission is LH or RH. Peak transmission for the left handed mode happens above the transmission zero and peak transmission for the right handed modes happens below the respective transmission zeros. This behavior is analogous to the one observed in, for example, planar transmission lines loaded with split ring resonators,[18] where composite dispersion characteristics can also be generated.

To summarize the above analysis, it was shown that the electromagnetic properties of the stacked holes arrays, which can be considered as fishnetlike devices, are dominated by different types of resonant features. This is in contrast to the first intuitive thought of a coupling mechanism driven by capacitive couplings between adjacent metallic layers.

V. CONCLUSION

Front side illuminated metamaterials can be fabricated by stacking subwavelength holes arrays. With respect to the previous demonstrations at millimeter waves, several points have been investigated, in particular the scaling to lower the dimensions of the holes size along with the periodicity, the dielectric spacer influence, and the fact of using elliptical

holes. These are found as the key parameters and permit one to push the operating frequencies in the terahertz range. The holes shape has a critical importance in the achievement of a high transmission level and can be optimized via the circuit approach analysis, whose validity is here demonstrated. This equivalent circuit can describe with a good accuracy the wide band transmission and reflection behavior of multilayer stacked holes arrays. Helpful in terms of design considerations, the equivalent circuit description is expected to provide further improvements including the design of low-loss broadband metamaterials, operating in a balanced composite mode.

ACKNOWLEDGMENTS

The authors thank Professor F. Medina (Univ. Seville, Spain) for valuable discussions. This work was carried out in the framework of a Delegation Générale pour l'Armement (DGA) contract. J. C. acknowledges the financial support of Spanish institutions, UPV through the PAI-2009 program and MICINN through Grant No. TEC 2007-67239 and Consolider under Grant No. CSD2008-00066.

[1]V. M. Shalaev, W. Cai, U. K. Chettiar, H.-K. Yuan, A. K. Sarychev, V. P. Drachev, and A. V. Kildishev, Opt. Lett. **30**, 3356 (2005).
[2]S. Zhang, W. Fan, K. J. Malloy, S. R. Brueck, N. C. Panoiu, and R. M. Osgood, Opt. Express **13**, 4922 (2005).
[3]J. Valentine, S. Zhang, T. Zentgraf, E. Ulin-Avila, D. A. Genov, G. Bartal, and X. Zhang, Nature (London) **455**, 376 (2008).
[4]M. Beruete, M. Sorolla, and I. Campillo, Opt. Express **14**, 5445 (2006).
[5]M. Beruete, I. Campillo, M. Navarro-Cía, F. Falcone, and M. Sorolla Ayza, IEEE Trans. Antennas Propag. **55**, 1514 (2007).
[6]C. Croënne, F. Garet, É. Lheurette, J. L. Coutaz, and D. Lippens, Appl. Phys. Lett. **94**, 133112 (2009).
[7]C. Caloz and T. Itoh, *Electromagnetic Metamaterials: Transmission Line Theory and Microwave Applications* (Wiley, New York, 2005).
[8]G. V. Eleftheriades and K. G. Balmain, *Negative-Refraction Metamaterials: Fundamental Principles and Applications* (Wiley-IEEE, Hoboken, New Jersey, 2005).
[9]F. Zhang, S. Potet, J. Carbonell, É. Lheurette, O. Vanbésien, X. Zhao, and D. Lippens, IEEE Trans. Microwave Theory Tech. **56**, 2566 (2008).
[10]F. Medina, F. Mesa, and R. Marqués, IEEE Trans. Microwave Theory Tech. **56**, 3108 (2008).
[11]R. Marqués, F. Mesa, L. Jelinek, and F. Medina, 2nd International Congress on Advanced Electromagnetic Materials in Microwaves and Optics (Metamaterials'2008), Symposium Digest, Pamplona, Spain, 23–26 September 2008.
[12]F. Medina, J. A. Ruiz-Cruz, F. Mesa, J. M. Rebollar, J. R. Montejo-Garai, and R. Marqués, Appl. Phys. Lett. **95**, 071102 (2009).
[13]R. Ortuño, C. García-Meca, F. J. Rodriguez-Fortuño, J. Martí, and A. Martínez, Phys. Rev. B **79**, 075425 (2009).
[14]L. Rayleigh, Proc. R. Soc. London, Ser. A **79**, 399 (1907).
[15]T. Li, J.-Q. Li, F.-M. Wang, Q.-J. Wang, H. Liu, S.-N. Zhu, and Y.-Y. Zhu, Appl. Phys. Lett. **90**, 251112 (2007).
[16]T. Li, H. Liu, F.-M. Wang, Z.-G. Dong, and S.-N. Zhu, Opt. Express **14**, 11155 (2006).
[17]R. Marqués, L. Jelinek, F. Mesa, and F. Medina, Opt. Express **17**, 11582 (2009).
[18]J. Carbonell, A. L. Borja, V. E. Boria, and D. Lippens, IEEE Antennas Wireless Propag. Lett. **8**, 886 (2009).